

Article

Advanced Operating Technique for Centralized and Decentralized Reservoirs Based on Flood Forecasting to Increase System Resilience in Urban Watersheds

Eui Hoon Lee 

School of Civil Engineering, Chungbuk National University, Cheongju 28644, Korea; hydrohydro@chungbuk.ac.kr; Tel.: +82-043-261-2407

Received: 13 June 2019; Accepted: 23 July 2019; Published: 24 July 2019



Abstract: The frequency of inundation in urban watersheds has increased, and structural measures have been conducted to prevent flood damage. The current non-structural measures for complementing structural measures are mostly independent non-structural measures. Unlike the current non-structural measures, the new operating technique based on flood forecasting is a real-time mixed measure, which means the combination of different non-structural measures. Artificial rainfall events based on the Huff distribution were used to generate preliminary and dangerous thresholds of flood forecasting. The new operation for centralized and decentralized reservoirs was conducted by two thresholds. The new operation showed good performance in terms of flooding and resilience based on historical rainfall events in 2010 and 2011. The flooding volume in the new operation decreased from 6617 to 3368 m³ compared to the current operation in 2010, and the flooding volume in 2011 decreased from 664 to 490 m³. In the 2010 event, the results of resilience were 0.831835 and 0.866566 in current and new operations, respectively. The result of resilience increased from 0.988823 to 0.993029 in the 2011 event. This suggestion can be applied to operating facilities in urban drainage systems and might provide a standard for the design process of urban drainage facilities.

Keywords: advanced operating technique; flood forecasting; urban drainage systems; resilience

1. Introduction

Global climate change is causing heavy rainfall, and unexpected heavy rainfalls have increased flooding in urban watersheds. It is important to take preemptive measures to prevent urban inundation owing to the enormous costs required for infrastructure restoration and damage to people and/or property when flooding events occur in urban areas. This study focuses on an improvement in the resilience of urban drainage systems using effective preemptive measures. Various structural measures (SMs) have been proposed, and most are costly and time consuming [1]. However, SMs such as the rehabilitation of urban drainage networks focused on the maximum overflow volume causing urban problems has been considered one of key elements for preventing urban inundation [2]. Non-structural measures (NSMs) are used to overcome the limitations of SMs because SMs have the effect of a designed capacity and cannot achieve an additional effect. Various measures including the operation of hydraulic facilities have been suggested, and those are categorized as NSMs. However, NSMs have been suggested individually, and independent NSMs can have a limited effect.

Various real-time control (RTC) techniques of hydraulic facilities have been classified as independent NSMs, NSMs combined with SMs (combined measures), and NSMs combined with the same type of NSMs (integrated NSMs). Most RTC techniques in urban areas are independent NSMs for urban drainage facilities [3–16]. Several studies such as combined measures have been introduced to increase the efficiency of urban drainage systems (UDSs) [1,17]. In addition, NSMs combined with the

same type of NSMs (operation technique with operation technique) have been suggested [1,16]. The operation technique applied in this study (mixed NSMs) suggests NSMs mixed with a different type of NSMs (the operation of drainage facilities based on a flood forecasting technique) [17,18]. Table 1 shows the classification of NSMs with RTC in UDSs.

Table 1. Classification of measures with real-time control (RTC) in urban drainage systems (UDSs). NSM, non-structural measure.

Measures	Studies
Independent NSMs	Beeneken et al. (2013) [3]; Cembrano et al. (2004) [4]; Fiorelli et al. (2013) [5]; Fuchs and Beeneken (2005) [6]; Galelli et al. (2012) [7]; Hsu et al. (2013) [8]; Kroll (2018) [9]; Lund et al. (2018) [10]; Pleau et al. (2005) [11]; Raimondi and Becciu (2015) [12]; Schütze et al. (2004) [13]; Vanrolleghem et al. (2005) [14]; Zacharof et al. (2004) [15]
Combined NSMs	Lee et al. (2017) [1]; Sweetapple et al. (2018) [16]
Integrated NSMs	Lee et al. (2016) [17]; Xu et al. (2018) [18]
Mixed NSMs	This study

Although many different studies on RTC in urban drainage systems have been suggested, the combination of different NSM such as operation of UDSs and flood forecasting has yet to be proposed. Furthermore, there are no mixed NSMs that can be applied to a small watershed at a minute scale in urban areas. In the urban watersheds of Korea, the concentration time is extremely short because most urban areas have a high impervious rate. The concentration time in an urban area is generally shorter than that of a rural area, and the concentration time in Korea is less than 1 h. Therefore, the rainfall will already have been discharged if the unit of time for RTC in an urban area exceeds 1 h. If the observed time interval is short in an urban watershed, the sophisticated management of UDSs will be possible. In this study, the unit of time for a flood forecasting and operation of UDSs is 1 min, the minimum unit of rainfall observation in Korea. The purpose of this study is the development of new mixed NSMs combining the operation of a drainage facility with flood forecasting to increase the system resilience in urban watersheds.

The concept of resilience in water resource engineering was suggested during the 2000s. Todini (2000) proposed an optimized design technique with two objective functions (cost and resilience) in a water distribution system [19]. A new reliability measure including network resilience with a genetic multi-objective approach was developed for the design of a water distribution system [20]. The multi-objective evolutionary algorithm was used for identifying the trade-off between the total cost and resilience including the reliability [21]. Earlier studies related to resilience in water resource engineering were conducted on water distribution systems. Studies on the resilience in UDSs have been introduced during the past several years. Mugume et al. (2015) introduced the use of structural resilience instead of reliability as a global analysis approach [22]. Decentralized stormwater management facilities have been applied to urban infrastructure for flexible and resilient systems [23]. The new operation technique based on flood forecasting described in this study is evaluated based on the system resilience. In this study, the various results according to the current operation, the previous operation, and the new operation in UDSs of the target watershed are evaluated.

In UDSs, there are two kinds of reservoirs such as centralized and decentralized reservoirs. Centralized reservoirs receive all inflow in the target watershed and discharge inflow using drainage pumps according to the constant water level. Decentralized reservoirs are reservoirs to prevent flood in subcatchments, and those are generally constructed in the underground of school playgrounds or children's parks. The current operation is the normal operation in centralized and decentralized reservoirs. The normal operation of centralized reservoirs means that drainage pumps are operated

according to predetermined water levels. The normal operation of decentralized reservoirs is to receive inflow and reserve inflow at the end of the rainfall event. The previous operation of centralized reservoirs is to change operation from the normal operation to the early operation according to the water level of the selected monitoring node. The normal operation of decentralized reservoirs is to receive inflow and reserve/discharge according to the water level of the selected monitoring node.

2. Methodologies

This study consisted of several major contents. First, artificial rainfall data were made using a Huff distribution with a proper quartile [24]. Second, an advanced flood forecasting technique was developed for RTC of drainage facilities and applied to a network in an urban drainage system. Third, an advanced operation technique based on the advanced flood forecasting technique was used for the urban drainage system (UDS) in the target watershed. Fourth, the new operation was compared with the current and previous operations to evaluate the resilience in the UDS. Figure 1 is the flow of this study.

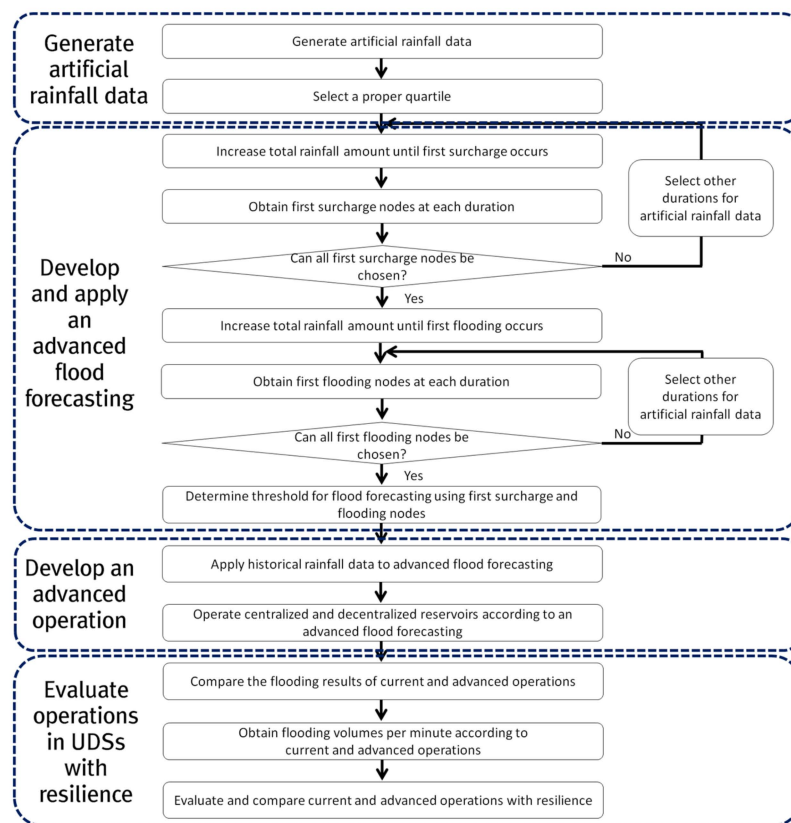


Figure 1. Flow of this study.

2.1. Production of Artificial Rainfall Data

In general, the UDSs in Korea are designed using artificial rainfall data distributed by a Huff distribution [24]. Huff (1967) observed the cumulative rainfall volume during historically heavy rainfall events and divided the total rainfall volume according to the location of the peak value. The Huff distribution has four quartiles, and it is categorized by the position of the peak value. The peak value of the first quartile is located between 0 and 0.25 T (Q1), where T is total rainfall duration. Each peak value of the second, third, and fourth quartiles is situated within 0.25–0.5 (Q2), 0.5–0.75 (Q3), and 0.75–1.00 T (Q4), respectively. Yoon et al. suggested Q3 for the design of hydraulic structures in Korea [25]. In this study, Q3 of the Huff distribution was selected for the generation of an advanced flood forecasting. All hydraulic structures in Korea were designed considering the design frequency of each hydraulic facility.

The hydraulic structures in Korea have different design frequencies. For example, the design frequency of a hydraulic structure is 30 years, and that of the B hydraulic structure is 20 years. Artificial rainfall data based on the Huff distribution was used to generate the preliminary and dangerous thresholds in the advanced flood forecasting. Historical rainfall events in 2010 and 2011 were used to check the operational effects because flood damage occurred in those periods.

Q1, Q2, Q3, and Q4 were non-dimensional using the cumulative rainfall volume and duration compared with the total rainfall volume and duration. Equations (1) and (2) show a non-dimensional rainfall volume and duration in a Huff distribution.

$$D(t) = \frac{CD(t)}{OD(t)} \times 100\% \tag{1}$$

$$R(t) = \frac{CR(t)}{OR(t)} \times 100\% \tag{2}$$

where $D(t)$ is the non-dimensional rainfall duration, $CD(t)$ is the cumulative rainfall duration, and $OD(t)$ is the total rainfall duration. In addition, $R(t)$ is the non-dimensional rainfall volume, $CR(t)$ the cumulative rainfall volume, and $OR(t)$ the total rainfall volume.

The Ministry of Construction and Transport in Korea has provided regression equations of a Huff distribution for 67 rainfall observatories managed by the Korea Meteorological Administration. The regression equations take the following form:

$$R(t) = C_0 + C_1D(t) + C_2D(t)^2 + C_3D(t)^3 + \dots + C_nD(t)^n \tag{3}$$

where C_n ($i = 1, 2, 3, \dots, n$) is the constant of the n th polynomial equation for a Huff distribution in each area. In Korea, a value of 6 is generally selected for n , although the value can be an integer of 5, 6, or 7. A process for applying non-dimensional cumulative rainfall into non-dimensional distributed rainfall is required. For example, the non-dimensional distributed rainfall volume at time i is $A - B$, when the non-dimensional cumulative rainfall volume at time i is A and at time $i - 1$ is B .

2.2. Advanced Flood Forecasting Technique

The flood forecasting technique using real-time rainfall data in an urban watershed was suggested by Lee et al. [26]. In the former study, the threshold for flood forecasting was generated using the first flooding nodes. The total rainfall volume in rainfall-runoff simulations was started at 1 mm and increased by 1 mm before the first flooding. Rainfall-runoff processes were simulated using a storm water management model (SWMM) [27]. The method suggested in the former study is extremely convenient and efficient in small urban watersheds. However, it is not a preemptive measure because the status of UDSs in the target area cannot be considered until the first flooding occurs. The advanced flood forecasting technique is generated by considering the surcharge of conduits in UDSs. This means that a threshold of proactive flood forecasting is added for preemptive measures. Figure 2 shows the concept of an advanced flood forecasting technique.

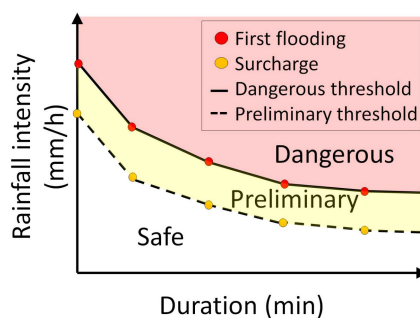


Figure 2. Concept of an advanced flood forecasting technique.

The preliminary and dangerous thresholds were generated differently according to the characteristics of each area. The application process of an advanced flood forecasting technique is shown in Figure 3.

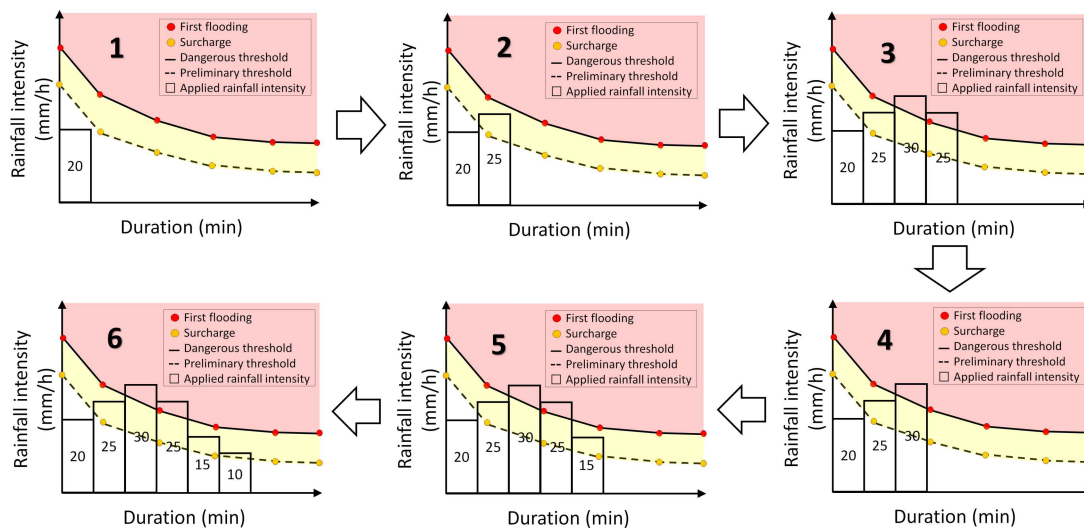


Figure 3. Application process of an advanced flood forecasting technique.

In the first step of Figure 3, real-time rainfall data were initially converted into the rainfall intensity and then applied to the advanced flood graph. The target area can be assumed to not be inundated if the applied rainfall intensity (ARI) is smaller than the preliminary and dangerous thresholds. The second rainfall intensity was added to the advanced flood graph and was over the preliminary threshold. In this step, a preemptive measure such as the early operation of the centralized reservoirs can be conducted to prevent the potential risk in UDSs. The early operation of the centralized reservoirs means that drainage pumps are operated earlier than the standard of the normal operation considering several required factors such as the required depth, head loss for the screen, the mechanical freeboard, and the bottom level of the centralized reservoir. This operation can reduce the backwater effect. In the former version, no flood forecasting was generated because the second rainfall intensity was not over the dangerous threshold. The process of the advanced flood forecasting from the third and fourth steps was similar to the former flood forecasting technique because the ARI was over the dangerous threshold. In the fifth and sixth steps, the ARI was located between the preliminary and dangerous thresholds. The short time interval of the ARI was appropriate for the advanced flood forecasting technique because the concentration time in an urban area is short. A regression equation should be applied to create an entire advanced flood graph when the rainfall duration is 0 min. A regression equation at 0 min can be applied without considering the rainfall observation interval. For example, a regression equation can be applied between 0 and 1 min, if the rainfall observation interval is 1 min. If the rainfall observation interval is 10 min, a regression equation can be generated between 0 and 10 min.

2.3. Advanced Operation for Centralized and Decentralized Reservoirs

The RTC technique between different drainage facilities in a drainage area was suggested and applied based on the status of the monitoring node [16]. In the former study, the results of flooding and system resilience applying historical rainfall events according to cooperative operating levels were suggested in a target area. UDSs can be prepared for an effective operation under heavy real-time rainfall events causing urban inundation if the operating standard of the urban drainage facilities (centralized and decentralized reservoirs) is based on the results of the flood forecasting. An advanced operation technique described herein was based on the rainfall intensity during an advanced operation.

An advanced operation for centralized and decentralized reservoirs applied in this study consisted of three steps according to the status of an advanced flood forecasting. A normal operation in a centralized reservoir was maintained, and reserved water in a decentralized reservoir was discharged to obtain the additional capacity if the applied rainfall data did not exceed two thresholds, namely the preliminary and dangerous thresholds. Initially, the centralized and decentralized reservoirs did not reserve water because the purpose of two reservoir was the prevention of urban inundation. The inflow volume could not be controlled because the inlet type of the decentralized reservoir was inlet weir. The rainfall event occurred, and the decentralized reservoir received water through the inlet weir. Additionally, the inflow volume in the centralized reservoir could not be controlled during the rainfall event, and drainage pumps were operated after the depth of the centralized reservoir reached the initial pump operating level. The range of operation in this study did not include this process, and it included the subsequent process.

The normal operation in a centralized reservoir was the operation of drainage pumps according to determined water levels in a centralized reservoir. Decentralized reservoirs have drainage pumps with small capacity because the capacity of drainage pumps is calculated by dividing the storage capacity in a decentralized reservoir by design discharge time, which is generally greater than 24 h. The reserved water in a decentralized reservoir is discharged by all drainage pumps. An early operation in a centralized reservoir was conducted to reduce the backwater effect, and the reserved water in a decentralized reservoir was discharged if the ARI was located between the two thresholds. If the ARI was over the dangerous threshold, the early operation in a centralized reservoir was maintained, and a decentralized reservoir did not discharge its reserved water. Figure 4 shows a schematic of an advanced operation in UDSs.

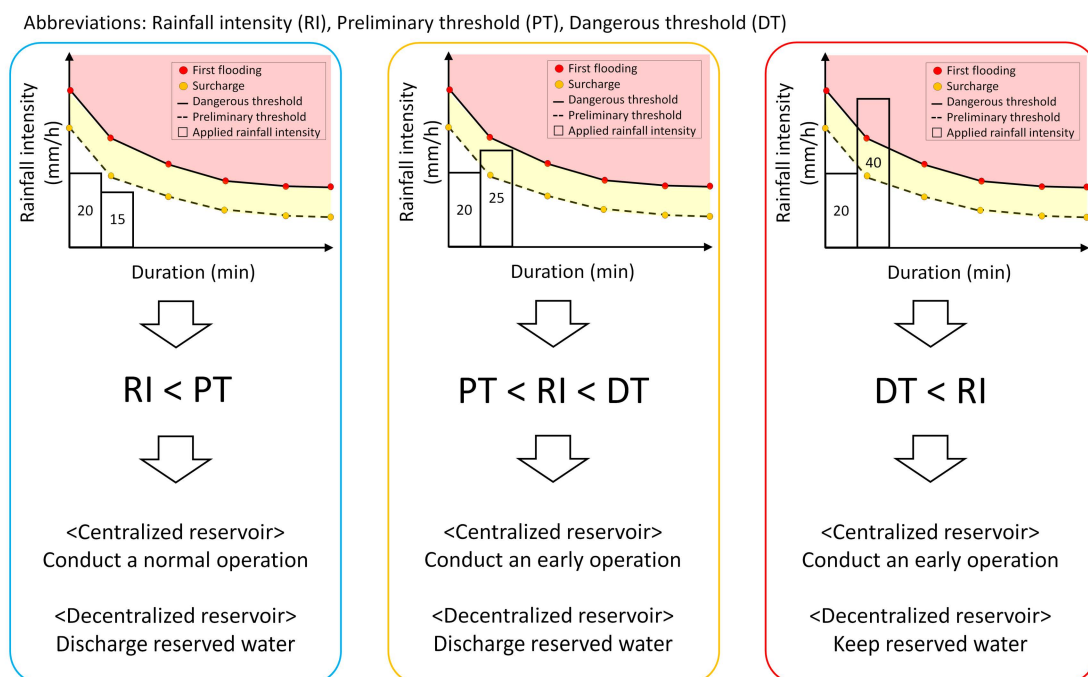


Figure 4. Schematic of an advanced operation in UDSs.

The initial pump operating level during an early operation in pump stations was determined by several factors. The first factor was the required depth, and the second factor was the head loss for screen. The third factor was the mechanical freeboard, and the fourth factor was the bottom level of the centralized reservoir. Other pump operating levels during an early operation in a centralized reservoir were calculated by considering the required depth [16].

2.4. Resilience of UDSs

To consider the status of UDSs over time, the resilience index was previously suggested [1,16]. In the previous studies, the performance evaluation function was determined by considering the total rainfall amount, basin area, and flood volume at each time. The system resilience is calculated based on the performance evaluation (PE) at each time. The difference between the two indices in the previous studies was based on the concentration time in the target area. The disadvantage of the two indices was that the denominator (total rainfall amount and basin area) of the PE function was so large that the value of the resilience of the UDS was close to 1, and there was no difference between the operations of UDS. In this study, the resilience index in a recent study was selected to evaluate the performance of the UDS [28]. The PE function is shown in Equations (4)–(6).

$$U(t) = \max\left(0, 1 - \frac{F(t)}{R(t) \times A}\right) \quad \text{subject to } F(t) \neq 0, R(t) \neq 0 \quad (4)$$

$$U(t) = 1 \quad \text{subject to } F(t) = 0 \quad (5)$$

$$U(t) = 0 \quad \text{subject to } F(t) \neq 0, R(t) = 0 \quad (6)$$

where $U(t)$ and $F(t)$ (m^3) are the value of the performance evaluation function and flood volume at time t , respectively. $R(t)$ (m) is the rainfall amount at time t , and A (m^2) is the basin area of the target watershed. The resilience of the UDS is calculated based on the value of the PE function in Equation (7).

$$Res(t) = \frac{1}{T} \int_0^{T=t \max} U(t) dt \quad (7)$$

where $Res(t)$ is the resilience of the UDS. The system resilience for each operation in the UDS at the study area can be calculated and compared.

3. Application and Results

3.1. Information of the Target Watershed

Seoul, the capital of Korea and the location of the study area, is one of the largest metropolitan cities in the world. Seoul is a basin-shaped city surrounded by mountains. The east-west distance of Seoul is 36.78 km, the north-south distance 30.3 km, and the area 605.25 km^2 . In addition, the area of Seoul is only 0.6% of the total area of Korea, and it has a high population density. The Han River penetrates from east to west in Seoul. Because Seoul is downstream of the Han River, the hydraulic gradient is gradually decreasing, and the flow of water is slow. In the case of flooding, the water level in Seoul (downstream from the Han River) is increased because of the water flowing from the upper and middle stream basin.

The target area is the drainage area of the Daerim3 pump station with a centralized reservoir in Yeongdeungpo-gu. Historical flood events in 2010 and 2011 occurred in Yeongdeungpo-gu, which is in the southeastern part of Seoul. The total amount and representative return period of the historical rainfall for the 2010 event are 256 mm and 100 years, respectively. The total amount and representative return period of the historical rainfall for the 2011 event are 386 mm and 100 years, respectively. The historical rainfall event in 2010 occurred from 20–21 September, and the historical rainfall event in 2011 occurred from 26–28 July. The total rainfall volume in 2010 was different from 2011, but the frequency in 2010 was the same as 2011 because the rainfall duration in 2010 was different from 2011.

The design return period of the Daerim3 pump station with a centralized reservoir is 30 years, and it has 12 drainage pumps (3411 m^3/min), while the capacity of the centralized reservoir is 33,650 m^3 . The design return period of the Daerim decentralized reservoir is 20 years, and it has 2 drainage pumps (18 m^3/min), while the capacity of a decentralized reservoir is 2477 m^3 . Table 2 shows the information on the centralized and decentralized reservoirs.

Table 2. Information on the centralized and decentralized reservoirs.

Drainage Facilities	Capacity of Reservoirs (m ³)	Capacity of Drainage Pumps (m ³ /min)	Boundary Conditions
Daerim3 pump station with a centralized reservoir	36,200	3411 (223 m ³ /min × 7, 150 m ³ /min × 1, 250 m ³ /min × 2, 600 m ³ /min × 2)	High water level: 9.0 m Low water level: 6.8 m
Daerim decentralized reservoir	2477	18 (9.0 m ³ /min × 2)	Total height: 3.2 m Inflow weir: 2 m × 0.4 m

The Seoul Metropolitan Government has provided Geographic Information System (GIS) data on all drainage areas in Seoul. An input network of SWMM using GIS data was generated. The number of subcatchments, junctions, and conduits was 1576, 1805, and 1977, respectively. The flow routing method was a dynamic wave, and the infiltration model was applied using Horton’s equation. The maximum rate, minimum rate, and decay constant in Horton’s equation at each sub-catchment were adjusted for the network calibration process. Figure 5 shows the information on the UDS used in the target watershed.

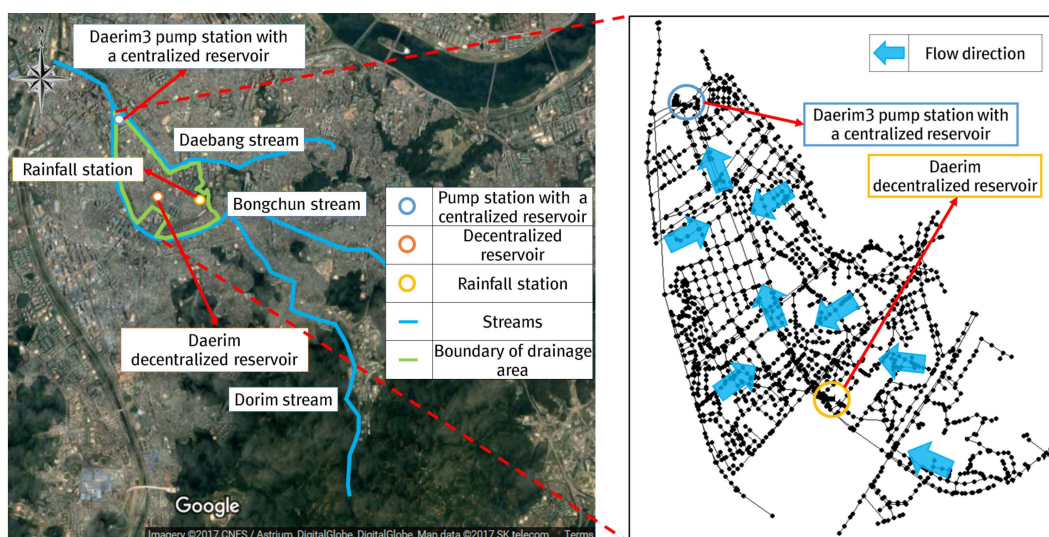


Figure 5. Information on the UDS used in the target watershed (Imagery © 2019 CNES/Airbus, DigitalGlobe, Landsat/Copernicus, NSPO 2019/Spot Image, Map data © SK telecom).

3.2. Application of Advanced Flood Forecasting

The artificial rainfall data distributed by the Huff distribution were applied for the rainfall-runoff simulation in the study area. The form of regression equations using the third quartile is shown in Equation (8).

$$R = 0.0005 - 0.3603D + 9.1084D^2 - 44.549D^3 + 105.18D^4 - 106.21D^5 + 37.835D^6 \quad (8)$$

where R is the non-dimensional rainfall volume and D is the non-dimensional rainfall duration. The rainfall amount was increased from 1 mm in 1-mm increments for each rainfall duration. For example, a rainfall amount of 50 mm was distributed through a Huff distribution and was applied to the rainfall-runoff simulation using SWMM. If a flood event did not occur, the rainfall amount can be increased to 51 mm. This process was repeated until the first flooding occurred. If flooding occurred, the rainfall amount could change to the intensity for the advanced flood forecasting in a target watershed. The artificial rainfall data were used for the generation of two thresholds (preliminary and

dangerous thresholds). The historical rainfall events in 2010 and 2011 were used to verify the effect of the new operation. The application of the historical rainfall event in 2010 is shown in Figure 6.

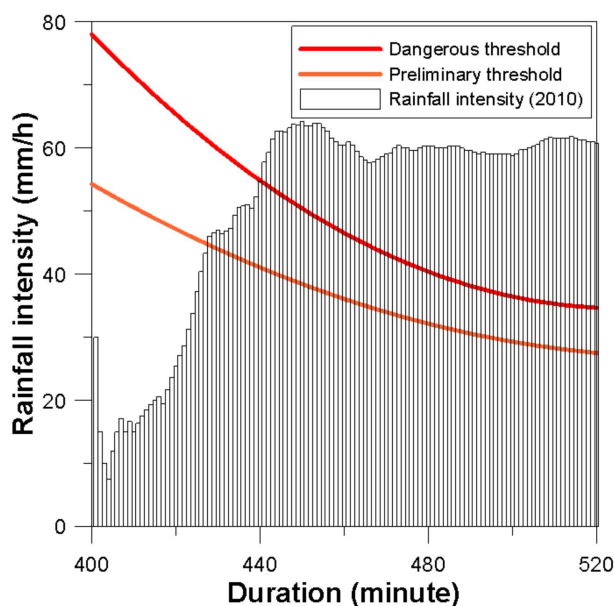


Figure 6. Application of the historical rainfall event in 2010.

A duration of 400–520 min was selected for the application of the advanced flood forecasting in 2010 because the rainfall intensity in other durations was lower than the preliminary threshold. The ARI in 2010 was larger than the preliminary threshold when the duration was 430 min and was greater than the dangerous threshold at 440 min. The proactive time in 2010 was obtained because the time difference between the preliminary and dangerous thresholds was 10 min. Within 430 min, an early operation of the centralized reservoir was applied, and the reserved water in the decentralized reservoir was discharged. Within 440 min, the early operation of the centralized reservoir was maintained, and the reserved water in the decentralized reservoir was stored. The early operation of centralized reservoirs was that drainage pumps were operated earlier than the standard of the normal operation considering several required factors such as the required depth, head loss for the screen, the mechanical freeboard, and the bottom level of the centralized reservoir. A very proactive time can be obtained based on meteorological forecasting. However, due to the time interval between meteorological forecasting and the operation of drainage facilities, it is difficult to combine with the operation of drainage facilities in small urban watersheds. Centralized reservoirs receive the inflow in urban watersheds, and drainage pumps are operated because the inflow is increased when a rainfall event occurs. Decentralized reservoirs receive water from the sewer network through an inlet weir when a rainfall event occurs. In the current operation, decentralized reservoirs reserve the received water without discharge until a rainfall event is finished. The application of the historical rainfall event in 2011 is shown in Figure 7.

A duration of 140–260 min was selected for the application of the advanced flood forecasting in 2011 because the rainfall intensity in the other duration was lower than the preliminary threshold. The ARI in 2011 was larger than the preliminary threshold when the duration was 150 min and was greater than the dangerous threshold at 155 min. The proactive time in 2011 was obtained because the time difference between the preliminary and dangerous thresholds was 5 min. Within 150 min, the early operation of the centralized reservoir was applied and the reserved water in the decentralized reservoir was discharged. Within 155 min, the early operation of the centralized reservoir was maintained and the reserved water in the decentralized reservoir was stored.

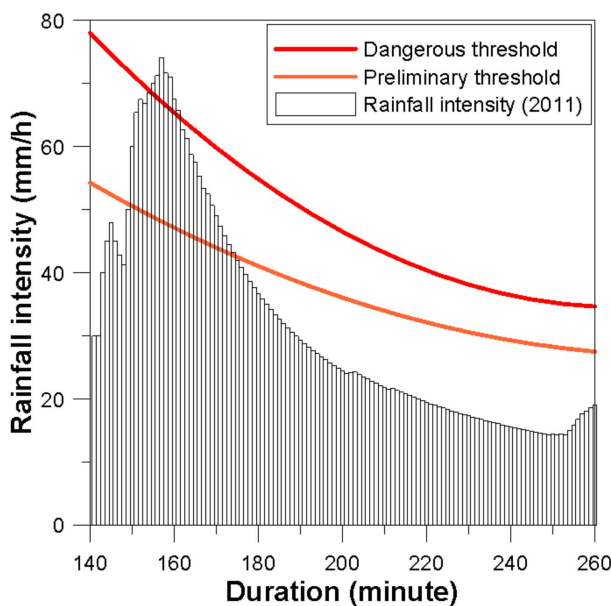


Figure 7. Application of the historical rainfall event in 2011.

3.3. Application of Advanced Operation for Centralized and Decentralized Reservoirs

The historical rainfall data of the past two years in 2010 and 2011 were used to compare the results of each operation. An advanced operation consists of the centralized and decentralized reservoir operations. The centralized reservoir operation is determined according to whether the ARI exceeds the preliminary threshold. If the ARI exceeds the preliminary threshold, the normal operation is changed to an early operation and vice versa in a centralized reservoir. The decentralized reservoir operation is determined according to whether the ARI exceeds the dangerous threshold. If the ARI exceeds the dangerous threshold, a normal operation is changed to an early operation and vice versa in a decentralized reservoir. If the ARI exceeds the dangerous threshold, the decentralized reservoir operation is changed from discharging the reserved water to maintaining it.

An early operation in a centralized reservoir was suggested in the previous study [28]. The determination of the initial pump operating level in centralized reservoirs is conducted to prevent a cavitation of drainage pumps. First, the required depth should be calculated, and it is calculated based on the initial pump capacity, the initial preparation time for pump, the required volume, and the mean area. The calculation of the required depth is shown in Equation (9).

$$D_R = (PT)/(4VA_m) \tag{9}$$

where D_R is the required depth, P is the initial pump capacity, and T is the initial preparation time for the pump. In addition, V is the required volume, and A_m is the mean area. The initial operating level is calculated using Equation (10).

$$O = D_R + H + F + B \tag{10}$$

where O is the initial pump operating level and H is the head loss for the screen. In addition, F is the mechanical freeboard, and B is the bottom elevation. The other operating levels can be calculated by considering the required depth in the centralized reservoir [16]. The operating level of the new operation was calculated using Equations (9) and (10). The operating levels during the normal and early operations of the centralized reservoir in the study area are listed in Table 3.

Table 3. Normal and early operation of the centralized reservoir in the study area [28].

Pump Station	Operation	Operating Level (m)												
		6.5	6.8	7.2	7.3	7.5	7.6	7.7	7.8	7.9	8.0	8.1	8.3	9.0
Daerim3	Normal	-	-	-	3.88	8.05	15.48	19.65	23.36	27.08	30.80	57.02	57.02	57.02
	Early	-	3.88	8.05	15.48	19.65	23.36	27.08	30.80	57.02	57.02	57.02	-	-

The results of applying the current operation, the previous operation [16] and the new operation to the historical rainfall event in 2010 are shown in Figure 8.

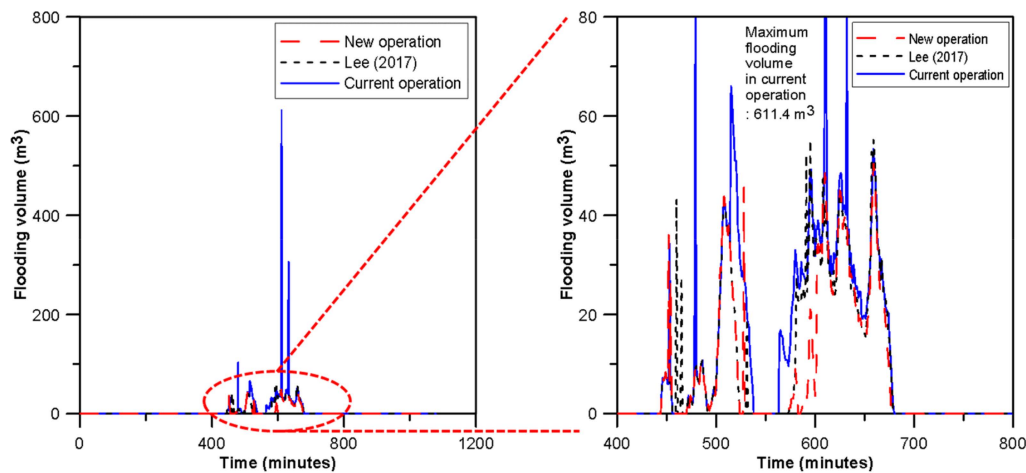


Figure 8. Flooding results of an advanced operation in 2010 [1].

The flooding volume according to each operation occurred between 400 and 700 min, as shown in Figure 8. The peak flooding volume (55.2 m^3) of the previous operation [16] was lower than that (611.4 m^3) of the current operation. Additionally, the advanced operation (new operation) showed the minimum peak value of flooding volume (50.4 m^3) among the three operations. The results of the total flooding volume during the current operation, previous operation, and new operation were 6617, 3904, and 3368 m^3 , respectively. The new operation showed a flooding reduction of 3249 m^3 compared to the current operation. The results of applying the current operation, previous operation, and new operation to the historical rainfall event in 2011 are shown in Figure 9.

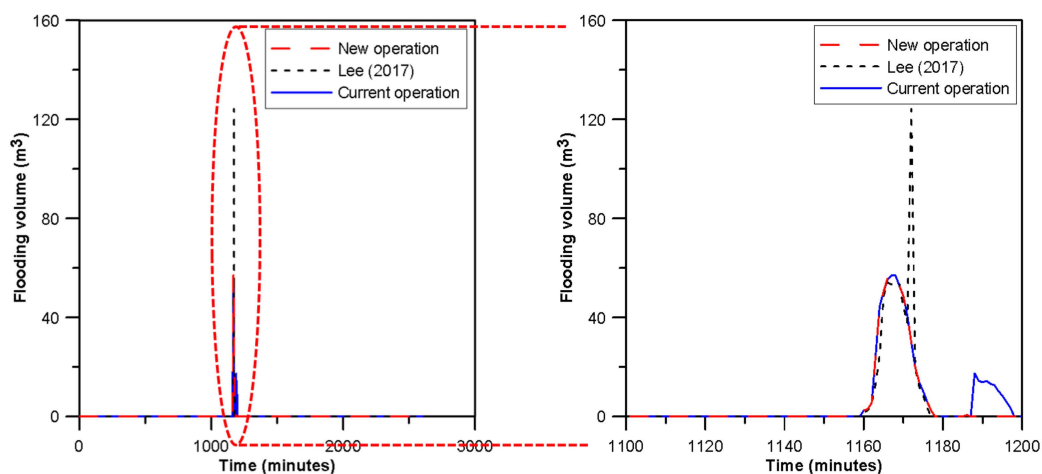


Figure 9. Flooding results of an advanced operation in 2011 [1].

The flooding volume according to each operation occurred between 1150 and 1200 min, as shown in Figure 9. The results in 2011 were different from those in 2010. The peak value of flooding volume (124.2 m^3) in the previous operation [16] was higher than that (57 m^3) in the current operation.

The current and advanced operation (new operation) showed the minimum peak flooding volume (57 m³). The previous operation showed the largest peak flooding volume among the three operations. The results of the total flooding volume during the current operation, previous operation, and new operation were 664, 552, and 490 m³, respectively. The new operation showed a flooding reduction of 174 m³ compared to the current operation. Diagrams with the reservoirs volume and discharge evolution are required. The volume and discharge in 2010 were selected because the flooding volume in 2010 was larger than 2011. The volume of the centralized reservoir in 2010 is shown in Figure 10.

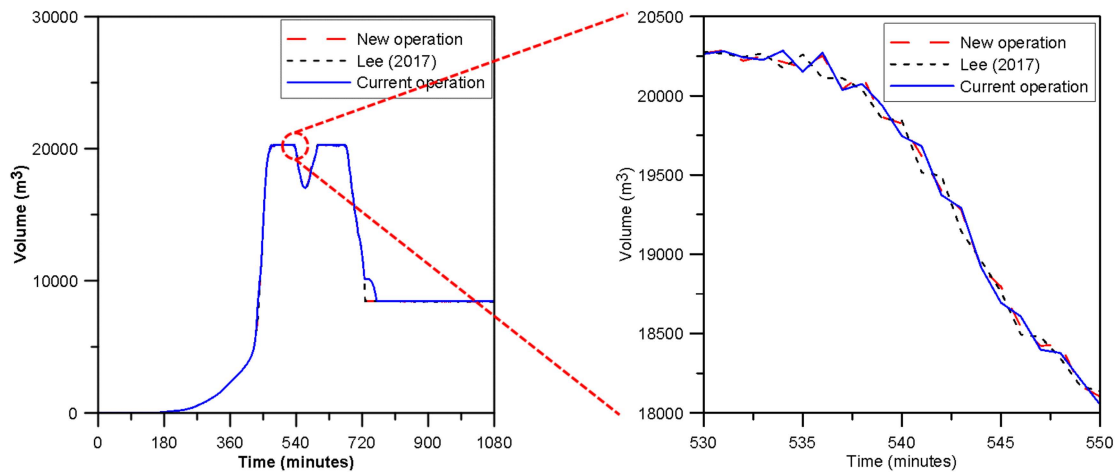


Figure 10. Volume of the centralized reservoir in 2010 [1].

There was a slight difference although the results of each operation were similar for the volume of the centralized reservoir in 2010. The obvious difference between each operation was found at about 720 min. There was no large difference between each operation because faster drainage in the centralized reservoir led to large inflow. The discharge of the centralized reservoir in 2010 is shown in Figure 11.

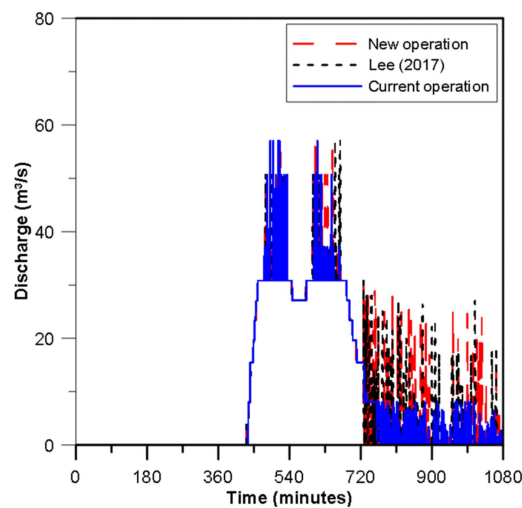


Figure 11. Discharge of the centralized reservoir in 2010 [1].

A clear difference between each operation was observed from 660 min. The new operation showed more discharge than the current operation. The volume of the decentralized reservoir in 2010 is shown in Figure 12.

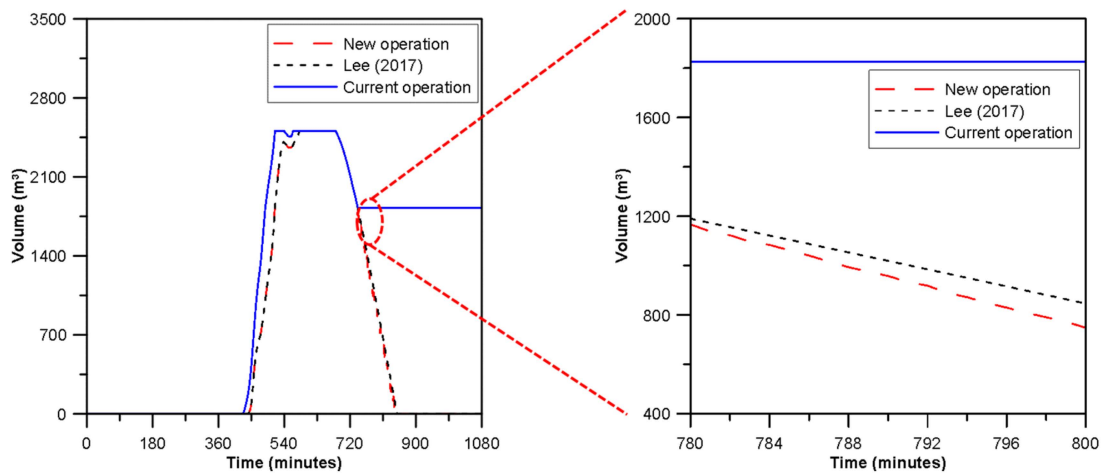


Figure 12. Volume of the decentralized reservoir in 2010 [1].

The difference of the volume in the decentralized reservoir according to each operation occurred at about 450 min. The biggest difference between the current and new operation occurred at about 750 min. In the new operation, the decentralized reservoir was completely empty at about 850 min, and it had additional capacity for continuous rainfall events. The discharge of the decentralized reservoir in 2010 is shown in Figure 13.

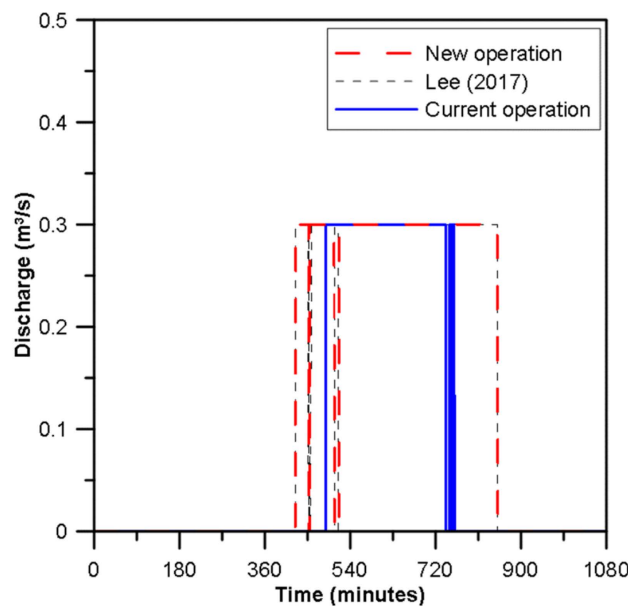


Figure 13. Discharge of the decentralized reservoir in 2010 [1].

A clear difference between each operation was observed from 660 min. The new operation showed more discharge than the current operation. The most important difference was that the discharge in the current operation stopped at 750 min, while the discharge in the new operation lasted up to 850 min.

3.4. Resilience of Advanced Operation with Advanced Flood Forecasting

The flooding volume in 2010 was more than that in 2011, and the duration of 2010 was shorter than that of 2011. This means that the flooding intensity (flooding volume per each duration) in 2010 was greater than that in 2011, and the system resilience of 2010 was lower than that of 2011. The results of the system resilience for each operation are shown in Table 4.

Table 4. Results of system resilience for each operation.

Event	System Resilience			
	Current Operation (1)	Previous Operation [16] (2)	New Operation (3)	Resilience Increment ((3) – (1))
2010	0.831835	0.855584	0.866566	0.034731
2011	0.988823	0.992997	0.993029	0.004206

The biggest difference in the system resilience for 2010 occurred when the current operation was changed to the new operation. The reason for the difference between the two operations was the existence of the early operation in the centralized reservoir and the additional capacity of the decentralized reservoir. The early operation in the centralized reservoir prevented a backwater effect by a safe and quick drainage in the UDS. The additional capacity in the decentralized reservoir can be obtained by the operation considering the level of conduits in the UDS.

The UDS in 2011 was relatively stable compared to that in 2010 because all system resilience exceeded 0.98. An operational difference occurred, although the urban drainage system showed a high system resilience during all operations. As with 2010, the difference between the two operations was caused by the reduction of the backwater effect in the centralized reservoir and the additional capacity of the decentralized reservoir.

4. Conclusions

The two non-structural measures proposed in this study were an advanced flood forecasting and an advanced operation for centralized and decentralized reservoirs. Advanced flood forecasting using real-time data of rainfall events is a technique to minimize the damage caused by flooding in urban areas as a preemptive non-structural measure. The advanced operation based on the advanced flood forecasting can maximize the efficiency by combining two individual non-structural measures (forecasting and operation). In addition, to evaluate the status of the UDS in the study area, the system resilience was applied to compare the current operation with the new operation.

The advanced flood forecasting and advanced operation proposed in this study can be systemized in various UDSs. It will be possible to apply the suggested technique in both small and large urban areas. In future studies, a threshold for flood damage in advanced flood forecasting can be added, making it possible to apply an advanced operation in various types of drainage facilities to large watersheds. Furthermore, customized flood forecasting and the operation of drainage facilities when considering the regional risk of flood damage may be suggested.

Author Contributions: E.H.L. carried out the survey of the previous studies, wrote the original manuscript, conducted the simulations, and conceived of the original idea of the proposed method.

Funding: This research was funded by the National Research Foundation (NRF) of Korea of the Korean government (NRF-2018R1C1B5086380).

Acknowledgments: This work was supported by a grant from The National Research Foundation (NRF) of Korea of the Korean government (NRF-2018R1C1B5086380).

Conflicts of Interest: The author declares no conflict of interest.

References

1. Lee, E.H.; Lee, Y.S.; Joo, J.G.; Jung, D.; Kim, J.H. Investigating the impact of proactive pump operation and capacity expansion on urban drainage system resilience. *J. Water Resour. Plan. Manag.* **2017**, *143*, 04017024. [[CrossRef](#)]
2. Gaudio, R.; Penna, N.; Viteritti, V. A combined methodology for the hydraulic rehabilitation of urban drainage networks. *Urban Water J.* **2016**, *13*, 644–656. [[CrossRef](#)]

3. Beeneken, T.; Erbe, V.; Messmer, A.; Reder, C.; Rohlfing, R.; Scheer, M.; Schuetze, M.; Schumacher, B.; Weilandt, M.; Weyand, M. Real time control (RTC) of urban drainage systems—A discussion of the additional efforts compared to conventionally operated systems. *Urban Water J.* **2013**, *10*, 293–299. [[CrossRef](#)]
4. Cembrano, G.; Quevedo, J.; Salamero, M.; Puig, V.; Figueras, J.; Marti, J. Optimal control of urban drainage systems. A case study. *Control Eng. Pract.* **2004**, *12*, 1–9. [[CrossRef](#)]
5. Fiorelli, D.; Schutz, G.; Klepiszewski, K.; Regneri, M.; Seiffert, S. Optimised real time operation of a sewer network using a multi-goal objective function. *Urban Water J.* **2013**, *10*, 342–353. [[CrossRef](#)]
6. Fuchs, L.; Beeneken, T. Development and implementation of a real-time control strategy for the sewer system of the city of Vienna. *Water Sci. Technol.* **2005**, *52*, 187–194. [[CrossRef](#)] [[PubMed](#)]
7. Galelli, S.; Goedbloed, A.; Schwanenberg, D.; van Overloop, P.J. Optimal real-time operation of multipurpose urban reservoirs: Case study in Singapore. *J. Water Res. Plan. ASCE* **2012**, *140*, 511–523. [[CrossRef](#)]
8. Hsu, N.S.; Huang, C.L.; Wei, C.C. Intelligent real-time operation of a pumping station for an urban drainage system. *J. Hydrol.* **2013**, *489*, 85–97. [[CrossRef](#)]
9. Kroll, S.; Fenu, A.; Wambecq, T.; Weemaes, M.; Van Impe, J.; Willems, P. Energy optimization of the urban drainage system by integrated real-time control during wet and dry weather conditions. *Urban Water J.* **2018**, *15*, 1–9. [[CrossRef](#)]
10. Lund, N.S.V.; Falk, A.K.V.; Borup, M.; Madsen, H.; Steen Mikkelsen, P. Model predictive control of urban drainage systems: A review and perspective towards smart real-time water management. *Crit. Rev. Environ. Sci. Technol.* **2018**, *48*, 1–61. [[CrossRef](#)]
11. Pleau, M.; Colas, H.; Lavallée, P.; Pelletier, G.; Bonin, R. Global optimal real-time control of the Quebec urban drainage system. *Environ. Model. Softw.* **2005**, *20*, 401–413. [[CrossRef](#)]
12. Raimondi, A.; Becciu, G. On pre-filling probability of flood control detention facilities. *Urban Water J.* **2015**, *12*, 344–351. [[CrossRef](#)]
13. Schütze, M.; Campisano, A.; Colas, H.; Schilling, W.; Vanrolleghem, P.A. Real time control of urban wastewater systems—Where do we stand today? *J. Hydrol.* **2004**, *299*, 335–348. [[CrossRef](#)]
14. Vanrolleghem, P.A.; Benedetti, L.; Meirlaen, J. Modelling and real-time control of the integrated urban wastewater system. *Environ. Model. Softw.* **2005**, *20*, 427–442. [[CrossRef](#)]
15. Zacharof, A.I.; Butler, D.; Schütze, M.; Beck, M.B. Screening for real-time control potential of urban wastewater systems. *J. Hydrol.* **2004**, *299*, 349–362. [[CrossRef](#)]
16. Sweetapple, C.; Astaraie-Imani, M.; Butler, D. Design and operation of urban wastewater systems considering reliability, risk and resilience. *Water Res.* **2018**, *147*, 1–12. [[CrossRef](#)] [[PubMed](#)]
17. Lee, E.H.; Lee, Y.S.; Joo, J.G.; Jung, D.; Kim, J.H. Flood reduction in urban drainage systems: Cooperative operation of centralized and decentralized reservoirs. *Water* **2016**, *8*, 469. [[CrossRef](#)]
18. Xu, W.D.; Fletcher, T.D.; Duncan, H.P.; Bergmann, D.J.; Breman, J.; Burns, M.J. Improving the multi-objective performance of rainwater harvesting systems using real-time control technology. *Water* **2018**, *10*, 147. [[CrossRef](#)]
19. Todini, E. Looped water distribution networks design using a resilience index based heuristic approach. *Urban Water J.* **2000**, *2*, 115–122. [[CrossRef](#)]
20. Prasad, T.D.; Park, N.S. Multiobjective genetic algorithms for design of water distribution networks. *J. Water Resour. Plan. Manag.* **2004**, *130*, 73–82. [[CrossRef](#)]
21. Farmani, R.; Walters, G.A.; Savic, D.A. Trade-off between total cost and reliability for Anytown water distribution network. *J. Water Resour. Plan. Manag.* **2005**, *131*, 161–171. [[CrossRef](#)]
22. Mugume, S.N.; Gomez, D.E.; Fu, G.; Farmani, R.; Butler, D. A global analysis approach for investigating structural resilience in urban drainage systems. *Water Res.* **2015**, *81*, 15–26. [[CrossRef](#)] [[PubMed](#)]
23. Siekmann, T.; Siekmann, M. Resilient urban drainage—Options of an optimized area-management. *Urban Water J.* **2015**, *12*, 44–51. [[CrossRef](#)]
24. Huff, F.A. Time distribution of rainfall in heavy storms. *Water Resour. Res.* **1967**, *3*, 1007–1019. [[CrossRef](#)]
25. Yoon, Y.N.; Jung, J.H.; Ryu, J.H. Introduction of design flood estimation. *J. Korea Water Resour. Assoc.* **2013**, *46*, 55–68.
26. Lee, E.H.; Kim, J.H.; Choo, Y.M.; Jo, D.J. Application of Flood Nomograph for Flood Forecasting in Urban Areas. *Water* **2018**, *10*, 53. [[CrossRef](#)]

27. United States Environmental Protection Agency. *Storm Water Management Model User's Manual Version 5.0*. EPA; United States Environmental Protection Agency: Washington, DC, USA, 2010.
28. Lee, E.H.; Choi, Y.H.; Kim, J.H. Real-Time Integrated Operation for Urban Streams with Centralized and Decentralized Reservoirs to Improve System Resilience. *Water* **2019**, *11*, 69. [[CrossRef](#)]



© 2019 by the author. Licensee MDPI, Basel, Switzerland. This article is an open access article distributed under the terms and conditions of the Creative Commons Attribution (CC BY) license (<http://creativecommons.org/licenses/by/4.0/>).